microorganisms

MDPI

Article

Survival of *Campylobacter jejuni* 11168H in *Acanthamoebae castellanii* Provides Mechanistic Insight into Host Pathogen Interactions

Fauzy Nasher *, Burhan Lehri, Megan F. Horney, Richard A. Stabler and Brendan W. Wren *

Faculty of Infectious and Tropical Diseases, London School of Hygiene and Tropical Medicine, London WC1E 7HT, UK

* Correspondence: fauzy.nasher1@lshtm.ac.uk (F.N.); brendan.wren@lshtm.ac.uk (B.W.W.)

Abstract: *Campylobacter jejuni* is the leading cause of bacterial foodborne gastroenteritis worldwide but is rarely transferred between human hosts. Although a recognized microaerophile, the majority of *C. jejuni* are incapable of growing in an aerobic environment. The persistence and transmission of this pathogen outside its warm-blooded avian and mammalian hosts is poorly understood. *Acanthamoebae* species are predatory protists and form an important ecological niche with several bacterial species. Here, we investigate the interaction of *C. jejuni* 11168H and *Acanthamoebae castellanii* at the single-cell level. We observe that a subpopulation of *C. jejuni* cells can resist killing by *A. castellanii,* and non-digested bacteria are exocytosed into the environment where they can persist. In addition, we observe that *A. castellanii* can harbor *C. jejuni* 11168H even upon encystment. Transcriptome analyses of *C. jejuni* interactions revealed similar survival mechanisms when infecting both *A. castellanii* and warm-blooded hosts. In particular, nitrosative stress defense mechanisms and flagellum function are important as confirmed by mutational analyses of *C. jejuni* 11168H. This study describes a new host–pathogen interaction for *C. jejuni* and confirms that amoebae are transient hosts for the persistence, adaptability, and potential transmission of *C. jejuni*.

Keywords: *Campylobacter jejuni*; *Acanthamoebae castellanii*; intra-amoebae; single-cell; host–pathogen interaction

Citation: Nasher, F.; Lehri, B.; Horney, M.F.; Stabler, R.A.; Wren, B.W. Survival of *Campylobacter jejuni* 11168H in *Acanthamoebae castellanii* Provides Mechanistic Insight into Host Pathogen Interactions. *Microorganisms* **2022**, *10*, 1894. https://doi.org/10.3390/microorganisms10101894

Academic Editor: Markus M. Heimesaat

Received: 15 August 2022
Accepted: 20 September 2022
Published: 23 September 2022

1. Introduction

Campylobacter jejuni is the most prevalent gastrointestinal bacterial pathogen worldwide but is rarely transferred between human hosts, suggesting that its high frequency in infection must relate to survival outside its warm-blooded hosts [1]. It is still ambiguous how this bacterium, an obligate microaerophile, remains omnipresent in the environment, given its inability to grow under atmospheric conditions [1,2]. Although not all 'environments' outside of the host may necessarily be aerobic, *C. jejuni* has been shown to form biofilms in atmospheric conditions as a mode of persistence [3,4] and has also been recognized to transform into a viable but non-culturable (VBNC) state [5,6]. This allows the bacterium to withstand many stresses and remain viable with low metabolic activity for months [7]. Additionally, several studies have investigated *C. jejuni's* environmental survival outside of the host with free-living protists [8–12]; however, the mechanistic understanding of this important niche remains poorly understood.

Free-living bacteria populations face constant challenges, particularly relating to predation by protists such as *Acanthamoebae* species [13–15]. Some bacteria have developed mechanisms to defend against killing within amoebic cells [14]. *Acanthamoebae* spp. have also been shown to have an important role in harboring and dissemination of pathogenic bacteria [13,14,16]. These interactions have been linked to several disease outbreaks of contaminated water [16] and food sources, including livestock [17]. *Acanthamoebae* spp. are characterized by a biphasic life cycle; a 'trophozoite' metabolically active form and

a 'cyst' state, which is a non-dividing dormant form [18]. Encystment occurs from the trophozoite form, with changes to the cell morphology including cell rounding and thicker cell wall [19]. The thickened cell wall enhances resistance to disinfection treatments and environmental stresses, which has been shown to be a reservoir for several intracellular bacteria pathogens [8,13,16,17].

Acanthamoebae spp. are widely used in research as non-mammalian surrogate organisms to study host interactions [20], including *C. jejuni* [11,12,21]. Studies have primarily focused on *C. jejuni*–amoebal interaction population measurements, which enumerate surviving bacteria by colony-forming units, but there is little information on *C. jejuni*–amoebae interactions at the single-cell level. Some studies have reported on the ability of *C. jejuni* to be phagocytosed by amoebae and thrive within this niche, where they multiply and "burst" out, leading to the release of *C. jejuni* into the environment [11]. This observation is seen in many other bacteria pathogens [14]. However, in our previous study we reported uptake of *C. jejuni* by *Acanthamoebae* spp. but not proliferation [12]. Instead, we observed that *Acanthamoebae* spp. are a transient host for *C. jejuni*, and survival of this bacterium within amoebae enhances its subsequent invasion and survivability in human epithelial cells and amoebae cells [12].

Here, we scrutinize the interaction of *C. jejuni* and *amoebae* using single-cell imaging complemented with intra-amoebal *C. jejuni* transcriptome profiling. We investigate the interaction of *C. jejuni* strain 11168H with *A. castellanii,* a keratitis strain from the T4 genotype, on the single-cell level by live-cell imaging using confocal microscopy. We show that sub populations of *C. jejuni* cells can (i) resist killing by *A. castellanii*; (ii) are released from *A. castellanii* through exocytosis; and (iii) contrary to previous reports [22], *C. jejuni* can maintain this niche upon amoebal encystment. *C. jejuni* genome is small (∼1.6 Mb), relative to other enteric pathogens [23,24]; therefore, we hypothesized that *C. jejuni* would use similar strategies to survive internalization by amoebae as it would with its warm-blooded hosts. Using RNA-Seq data and mutagenesis we show that *C. jejuni* 11168H indeed utilizes similar strategies to survive and persist within amoebae as it does with its warm-blooded hosts. Our data reinforce the observation that *A. castellanii* are an important transient host for *C. jejuni* 11168H and may enhance environmental persistence of this prevalent pathogen.

2. Materials and Methods

2.1. Strains and Cultures

Campylobacter jejuni strain 11168H, a motile derivative of the original sequence strain NCTC 11168 [25], were stored using Protect bacterial preservers (Technical Service Consultants, England, UK) at −80 °C. Bacteria were streaked on Columbia blood agar (CBA) plates containing Columbia agar base (Oxoid) supplemented with 7% (*v*/*v*) horse blood (TCS Microbiology, UK) and grown at 37 °C in a microaerobic chamber (Don Whitley Scientific, England, UK), containing 85% N_2, 10% CO_2, and 5% O_2 for 48 h. Bacteria were grown on CBA plates for a further 16 h at 37 °C prior to use.

Acanthamoeba castellanii (T4 genotype) Culture Collection of Algae and Protozoa (CCAP) 1501/10 (Scottish Marine Institute) were grown to confluence at 25 °C in 75-cm^2 tissue culture flasks containing peptone yeast and glucose (PYG) media (proteose peptone 20 g, glucose 18 g, yeast extract 2 g, sodium citrate dihydrate 1 g, $MgSO_4 \times 7H_2O$ 0.98 g, $Na_2HPO_4 \times 7H_2O$ 0.355 g, KH_2PO_4 0.34 g in distilled water to make 1000 mL, pH was adjusted to 6.5). Amoebae were harvested by scraping the cells into suspension, and viability was determined by staining with trypan blue and counting by a hemocytometer using inverted light microscopy.

2.2. C. jejuni Mutant Transformation

C. jejuni 11168H mutant constructs were obtained from the Campylobacter Resource Facility (http://crf.lshtm.ac.uk/wren_mutants.htm, accessed on 1 August 2022) and strain 11168H was naturally transformed using the previously described biphasic method [26]

with some minor changes. Briefly, *C. jejuni* was cultured on Mueller Hinton (MH) agar for 16 h, cells were resuspended in MH broth to an OD_{600nm} = 0.5, 0.5 mL of this suspension was added to a 15 mL falcon that contained 1 mL of MH agar, *C. jejuni* donor DNA 0.1–1 µg was added to the suspension and incubated for 24 h at 37 °C in microaerobic conditions, and the suspension was plated on MH agar with respective antibiotic for up to 5 days. *C. jejuni* green fluorescent producing bacteria (GFP) strain $11168H_{GFP}$ was constructed as previously described [12,27]. *C. jejuni* constructs 11168HΔ*cgb*, 1168HΔ*dsbA,* and 1168HΔ*dsbB* were a gift from Dr. Aidan. J. Taylor (University of Sheffield). All strains used in the study can be found in Supplementary File S1 (Table S2).

2.3. C. jejuni Invasion and Survival Assay

Invasion and survival assays were performed as previously described [12,28] with minor alterations. Briefly, *C. jejuni* 11168H and its mutants were incubated with a monolayer of approximately 10^6 *A. castellanii* at a multiplicity of infection (M.O.I) of 200:1 for 3 h at 25 °C in 2 mL PYG media (the M.O.I. of 200:1 was chosen to allow maximal internalization of bacteria without impacting amoebae predation through density-dependent inhibition). The monolayer was washed 3× with phosphate buffer saline solution (PBS) and incubated for 1 h in 2 mL of PYG media containing 100 µg/mL of gentamicin. *C. jejuni* cells were harvested by scraping the amoebae into suspension and centrifuged for 10 min at 350× *g* to pellet the bacteria and amoebae. Supernatant was discarded and the pellet was suspended in 2 mL of distilled water containing 0.1% (*v*/*v*) Triton X-100 for 10 min at room temperature with vigorous pipetting (every 2 min) to lyse the amoebae and release bacteria cells. The suspension was then centrifuged for a further 10 min at 4000× *g*, the resultant pellet was resuspended in 1 mL PBS and enumerated for colony forming units on CBA plates for up to 72 h at 37 °C microaerobically.

2.4. Live-Cell Imaging

Green fluorescent protein (GFP) producing *C. jejuni* $11168H_{GFP}$ strain was used for confocal live-cell imaging. Time lapse experiments were performed as described above with minor changes. *A. castellanii* cells were incubated in PYG media supplemented with dextran-conjugated Texas Red (10,000 MW; Thermofischer) at a final concentration of 100 µg/mL overnight. *A. castellanii* cells were washed three times and approximately 10^6 of adherent amoebae were infected with *C. jejuni* $11168H_{GFP}$ (M.O.I of 200) in 35 mm µ-Dish devices (IBIDI) prior to imaging. Texas Red-conjugated dextran was monitored in the red region (excitation and emission wavelengths are 595/615 nm) and GFP was monitored in the green region (excitation and emission wavelengths are 488/510 nm).

Confocal laser scanning microscopy images were obtained using an inverted Zeiss LSM 880 confocal microscope (Zeiss, Berlin, Germany). Images were taken at 5 s intervals for time lapse experiments.

2.5. RNA-Seq and Real-Time RT-qPCR

RNA-Seq was used to identify differentially expressed genes between intra-amoebal *C. jejuni* strain 11168H and the control (which was incubated in the absence of *A. castellanii*) after a total of 4 h. Experiments were performed as described above; briefly, *A. castellanii* 10^6 were infected co-incubated with *C. jejuni* 11168H (M.O.I of 200) for 3 h and washed three times to remove extracellular bacteria. Gentamycin was added to a final concentration of 100 µg/mL; this culture was incubated for a further 1 h before washing three times and RNA was extracted using Triazole (Sigma Aldrich, England, UK) following manufacturer's protocol. Ribosomal RNA was depleted using Ribominus (Invitrogen, Scotland, UK), and libraries were prepared using TruSeq® Stranded mRNA (Illumina, Carlifonia, US). Raw reads were obtained from an Illumina MiSeq paired-end sequencing platform (Illumina). The paired-end reads were trimmed and filtered using Sickle v1.200 [29]; Bowtie2 [30] was used to map the reads against the reference sequence, *C. jejuni* strains 11168H assembly GCA_900117385.1. Cufflinks suite [31] was used to convert annotations from GFF

to GTF format, and Bedtools [32] was used to generate transcript counts per samples. Statistical analysis was performed in R using the combined data generated from the bioinformatics as well as metadata associated with the study (multifactorial design). Adjusted *p*-value significance cut-off of 0.001, and log fold change cut-off of >1.5, was used for multiple comparison.

Expression of genes of interest were quantified by real-time RT-qPCR and normalized against *gyrA*. A 1 µg of total RNA of each sample was reverse-transcribed to cDNA using RT^2 first strand kit (Qiagen) according to manufacturer's protocol. Quantification of gene expression was achieved by real-time RT-qPCR using $Sybr^{TM}$ Green real-time PCR master mix using primers generated using PrimerQuest (IDT) (Supplementary File S1 (Table S3)). Real-time RT-PCR was performed in 96-well plates using an ABI PRISM 7300 Real-time PCR System (Applied Biosystems), and the relative gene expression for the different genes was calculated from the crossing threshold (Ct) value according to the manufacturer's protocol ($2^{-\Delta\Delta Ct}$) after normalization using the *gyrA* endogenous control (68).

2.6. Statistical Analysis

Evaluation of *C. jejuni* interaction with *A. castellanii* was based on at least 500 amoebae cells per experiment. All experiments presented are at least three independent biological replicates. RNA-Seq analysis were performed in R using the combined data generated from the bioinformatics. Differentially expressed genes were considered significant when the *p*-value of three independent biological experiments was below 0.001. All other data were analyzed using Prism statistical software (Version 9, GraphPad Software, San Diego, CA, USA), and statistical significance was considered when the *p*-value was <0.05. All values are presented as standard deviation of at least three independent experiments.

3. Results

3.1. Undigested C. jejuni Are Released Back into the Environment

As a predator, free-living amoebae inhabits aquatic environments, a niche often occupied by *C. jejuni* [9,19,20]. It is plausible that these two organisms have frequent encounters and have co-evolved. Using green fluorescent protein (GFP) producing *C. jejuni* strain 11168H ($1168H_{GFP}$) and indigestible-conjugated dextran to track the phago–endosomal pathway time-lapse imaging (0–3.5 h post infection (h.p.i)), we studied the interaction of *C. jejuni* and *A. castellanii* at the single-cell level. We observed internalization, trafficking of bacteria into digestive vacuoles, and the persistence of undigested *C. jejuni* (Figure 1).

To identify the compartment containing intracellular *C. jejuni*, we followed the time-course of the phago–endosomal pathway by incubating amoebae for 16 h with indigestible fluorophore conjugated to a complex branched glucan, dextran-Texas Red, and tracked localization. In line with a previous study [8], we observed aggregation of *C. jejuni* 11168H at a certain position on *A. castellanii* prior to entering the amoebae. This aggregation phenotype was termed "backpack" formation [33] (Figure 1a); we also observed formation of small bacteria-filled vacuoles (Figure 1b), which ultimately formed larger compartments that colocalized with dextran; this indicated that intracellular *C. jejuni* are trafficked into "digestive-vacuoles" (Figure 1c,d).

Whilst most of the *C. jejuni* were lysed within these compartments, a fraction of the bacteria survived. This was based on retained integrity of the classical helical-shape morphology of *C. jejuni*. Next, we sought to observe the fate of these intact *C. jejuni* cells within these compartments (Figure 2).

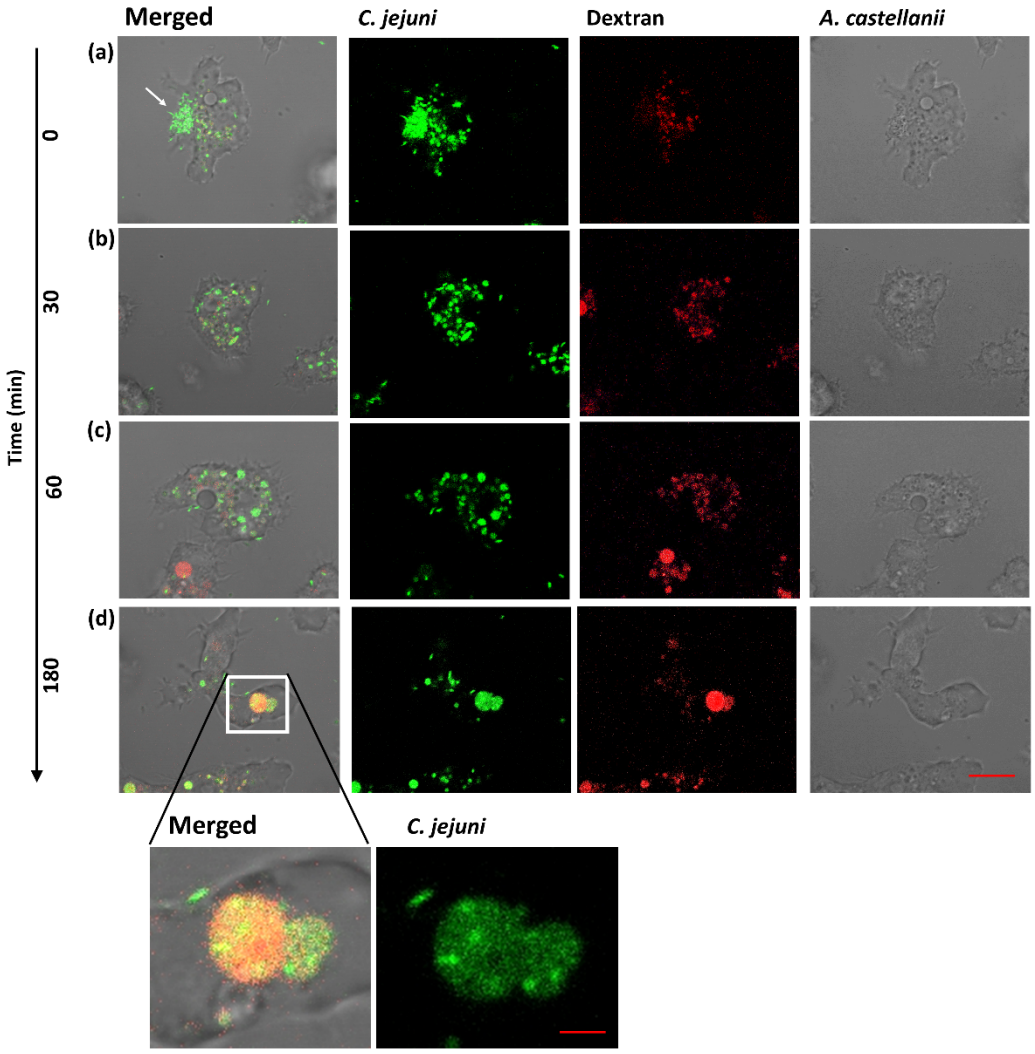

Figure 1. Single cell time-lapse imaging with confocal microscopy monitoring the interaction of *A. castellanii* and *C. jejuni* 11168H. (**a**) uptake of *C. jejuni* by *A. castellanii* (indicated by arrow); (**b**) internalized *C. jejuni* form small bacteria-filled vacuoles; (**c**) the small bacteria-filled vacuoles fuse to form larger vacuoles; and (**d**) *C. jejuni* colocalizes with Texas Red-conjugated dextran within vacuolar compartments of *A. castellanii* at ∼3 h.p.i. (inset; shows fusion of bacteria-filled vacuole with dextran-filled vacuole). The amoebae are visible in the transmitted-light channel (labeled: *A. castellanii*); GFP-producing *C. jejuni* 11168H$_{GFP}$ in the green channel (labeled: *C. jejuni*); merged signals are shown on the right (labeled: Merged); dextran-filled vacuole labeled with Texas Red-conjugated dextran in the red channel (labeled: Dextran). Representation of three independent biological replicates; images were captured with ×63 oil objective, 5 s intervals. Time is indicated on the left (min). Scale bar: 10 µm and 2 µm for inset.

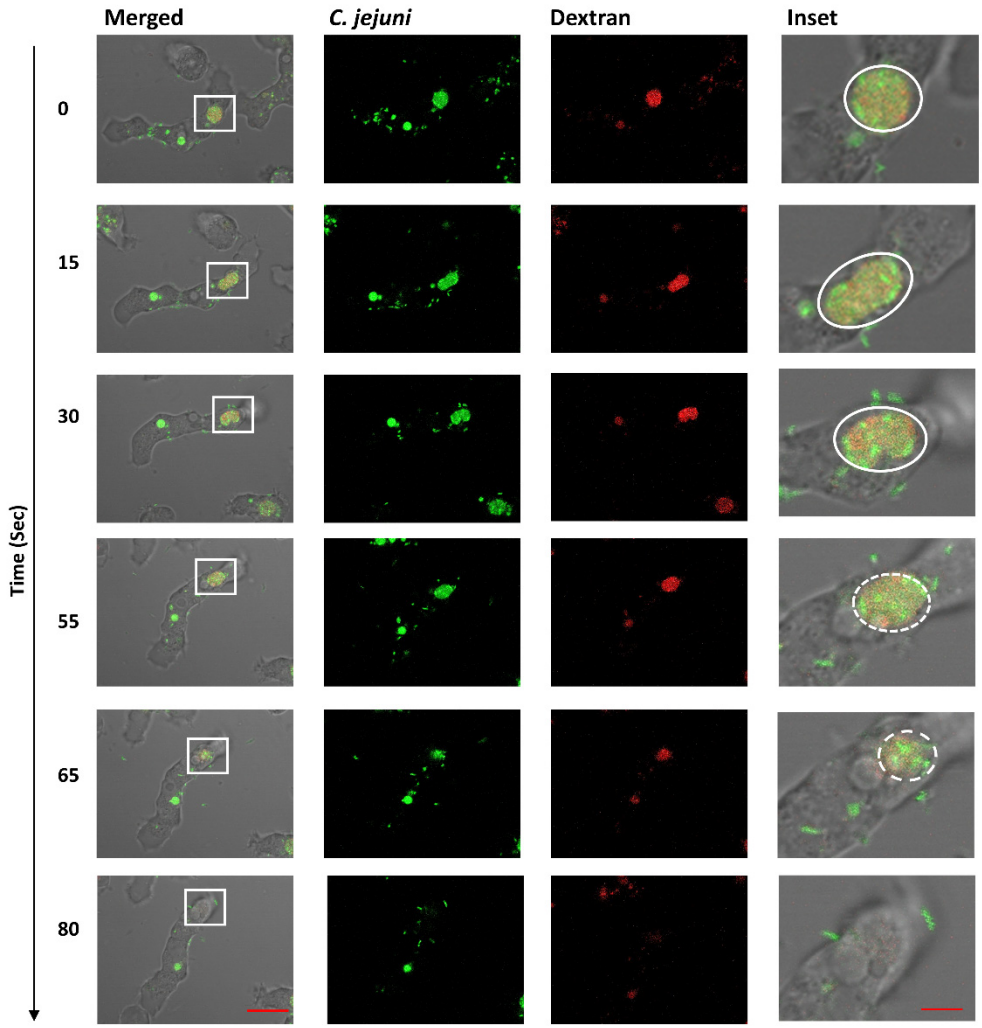

Figure 2. Time-lapse imaging with confocal microscopy showing exocytosis of *C. jejuni* colocalized with dextran. GFP-producing *C. jejuni* 11168H were incubated with *A. castellanii* for 3.5 h and then monitored over a period of 80 s (relative time shown on the left). Images represent merged transmitted-light (amoebae); GFP channels (*C. jejuni*); red channels (dextran). The inset shows magnification of the white-boxed areas: highlighted with a circle/oval shows an intact compartment; dashed circle/oval indicate release of vacuole content. Representation of three independent biological replicates; images were captured at ×63 oil objective at 5 s intervals. Time is indicated on the left (in seconds). Scale bars: 10 µm; and 2 µm for inset image. See Supplementary Movie S1.

A. castellanii were incubated with *C. jejuni* 11168H$_{GFP}$ for 3.5 h and monitored over a period of 80 s. Live-cell imaging revealed that these undigested bacteria are exocytosed back into the environment (Figure 2 and Supplementary Movie S1). Similar to other phagocytes [34,35], *A. castellanii* accumulated cellular waste, such as digested bacteria, and the dextran are excreted out of the cell, thus also releasing undigested bacteria back into the environment. We did not observe this phenotype using a non-pathogenic *E. coli* strain DH5α tagged with the fluorophore mCherry (Supplementary File, Figure S2).

3.2. *C. jejuni* Maintains a Niche within Amoebic Cyst

Contrary to previous reports [11,21,28], we did not observe intracellular multiplication of *C. jejuni* 11168H and lysis of amoebae, but we did observe *C. jejuni 11168H*$_{GFP}$ within the cyst form of *A. castellanii* (Figure 3).

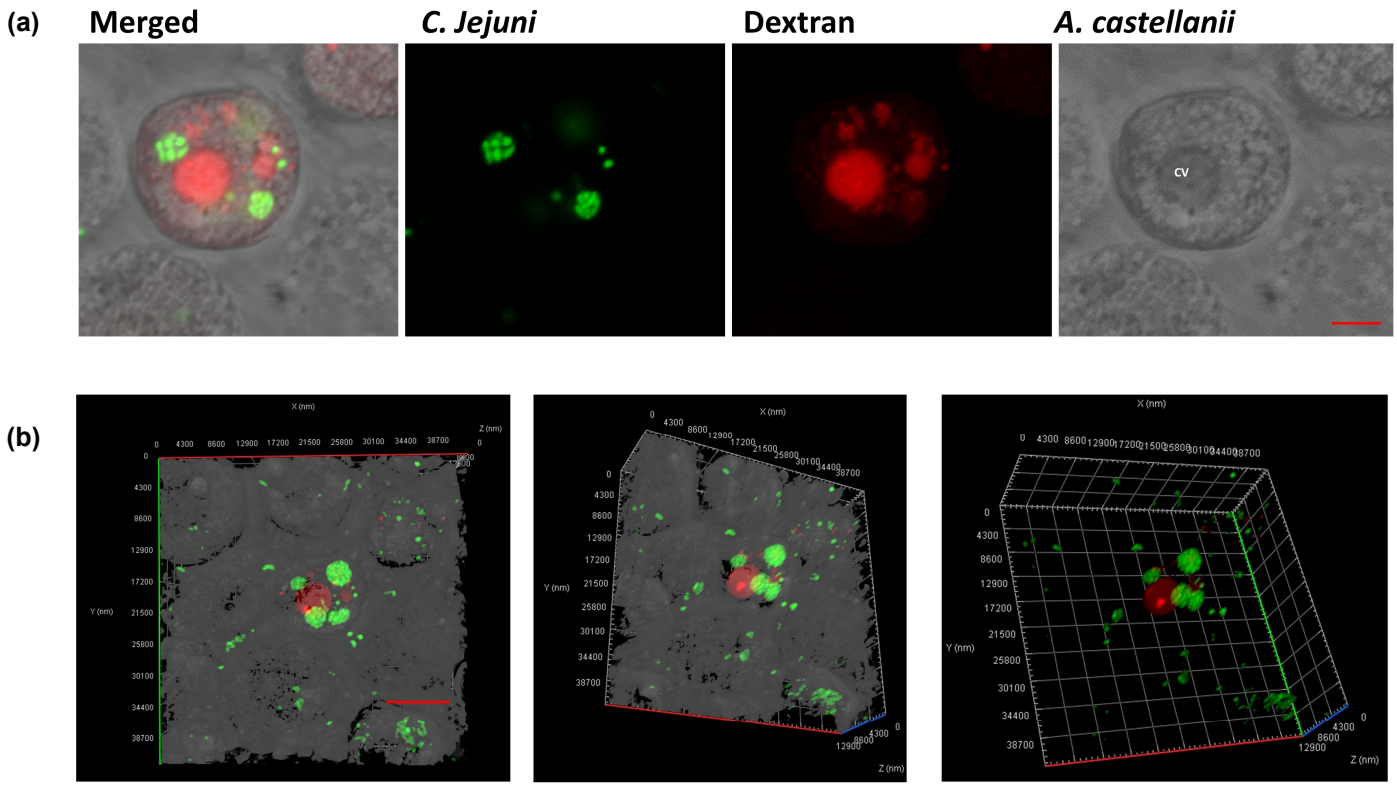

Figure 3. ***C. jejuni 11168H*$_{GFP}$ within *A. castellanii* cyst.** GFP-producing bacteria were incubated with *A. castellanii* (M.O.I 1:200) for 72 h and imaged with confocal microscopy, (**a**) internalized *C. jejuni* are localized in small, tightly packed compartments. The amoebae are visible in the transmitted-light channel (labeled: *A. castellanii*); GFP-producing *C. jejuni* 11168H$_{GFP}$ in the green channel (labeled: *C. jejuni*); merged signals (labeled: Merged); and Texas Red-conjugated dextran filled compartments are shown with the Red channel (labeled: Dextran); CV = contractile vacuole; (**b**) volume view of confocal Z-stack showing tightly packed compartments filled with GFP-producing *C. jejuni* (Green); and Texas Red-conjugated dextran filled compartment. Images were captured with ×63 oil objective Scale bar: 5 µm. A representation of three biological replicate, *n* = 500 amoebic cysts were counted per experiment.

C. jejuni 11168H$_{GFP}$ was incubated with *A. castellanii* for 72 h at 25 °C in PYG media before imaging with confocal microscopy. Out of 500 amoebic cysts that were enumerated in each biological replicate, an average of ∼30% contained GFP-producing bacteria (Figure 3a,b). Previously, it was reported that intracellular survival of *C. jejuni* undergoes drastic physiological changes, and recovery required pre-culturing under oxygen-limiting conditions (anaerobic) [36]; however, we were unable to recover viable colony forming units (cfu) from this culture. This suggested that *C. jejuni* 11168H may undergo metabolic reprogramming within *A. castellanii* cysts.

3.3. Intra-Amoebal C. jejuni Transcriptome

To identify the key regulatory changes triggered by survival of *C. jejuni* within *A. castellanii*, RNA-Seq was used to determine differentially expressed genes in strain 11168h intra-amoebae relative to the control at 4 h post infection. There was a large difference in gene expression between intra-amoebae *C. jejuni* and the control; a total of 94 genes were differentially transcribed (>1.5-fold; *p*-value < 0.001): 72 were up-regulated whilst 22 were down-regulated in the intra-amoebae *C. jejuni* (Table 1).

Table 1. Significantly differentially expressed genes in intra-amoebae *C. jejuni* compared to the control in strain 11168H after 4 h post infection.

Upregulated				
Gene ID	**Gene Name**	**Description of Product**	**Log^2 Fold Change**	**Adjusted *p*-Value**
Cj1586	*cgb*	Single domain hemoglobin	4.663339	1.88×10^{-26}
Cj0974		Uncharacterized protein	4.417067	6.57×10^{-5}
Cj1340c	*Maf1*	Motility accessory protein	4.349186	6.28×10^{-34}
Cj0380c		Uncharacterized protein	4.241269	1.77×10^{-4}
Cj0972		Uncharacterized protein	4.14400	1.08×10^{-5}
Cj0758	***grpE***	**Response to hyperosmotic and heat shock**	**3.963416**	**1.38×10^{-20}**
Cj0971		**Uncharacterized protein**	**3.459789**	**2.23×10^{-4}**
Cj0241c	*herA*	**Bacteriohemerythrin**	3.326818	1.75×10^{-2}
Cj0877c		Uncharacterized protein	3.258874	3.88×10^{-3}
Cj0200c		Periplasmic protein	3.249386	$6.69 \times 10-^{12}$
Cj1650	*fliS*	Flagellar export chaperone [37]	3.201313	3.33×10^{-19}
Cj0836	***ogt***	**Methyltransferase**	**2.961825**	**2.21×10^{-13}**
Cj1242	***ciaC***	**Campylobacter Invasion antigen C**	**2.946553**	**5.82×10^{-38}**
Cj0201c	*imB*	Integral membrane protein	2.902751	6.00×10^{-3}
Cj0921c	***peb1A***	**Amino acid transporter**	**2.902712**	**2.54×10^{-24}**
Cj0865	***dsbB***	**Protein-disulfide oxidoreductase**	**2.727325**	**9.52×10^{-11}**
Cj0030		Uncharacterized protein	2.711549	7.47×10^{-25}
Cj1465	*flgN*	Flagellar hook protein [38]	2.704280	5.90×10^{-12}
Cj0251c		Highly acidic protein	2.676403	1.56×10^{-5}
Cj0829c		Uncharacterized protein (Putative CoA binding domain containing protein)	2.664411	1.76×10^{-5}
Cj1503c	*putA*	Putative proline dehydrogenase/delta−1-pyrroline-5-carboxylate dehydrogenase	2.646897	9.64×10^{-54}
Cj1537c	*acsA*	Acetyl-coenzyme A synthetase	2.643273	9.49×10^{-16}
Cj0243c		Uncharacterized protein	2.508166	5.98×10^{-6}
Cj1450	***ciaI***	**Putative ATP/GTP-binding protein**	**2.461822**	**3.79×10^{-17}**
Cj0919c		Aspartate/glutamate/glutamine transport system permease protein	2.401703	7.08×10^{-10}
Cj0459c		Uncharacterized protein	2.291369	5.87×10^{-13}
Cj1075	*fliW*	Flagellar assembly factor	2.260313	3.55×10^{-8}
Cj0018c	*dba*	Disulfide bond formation protein	2.260119	1.52×10^{-6}
Cj1668c		Periplasmic protein	2.168892	2.44×10^{-10}
Cj0967		Periplasmic protein	2.103994	1.08×10^{-4}
Cj1682c	*gltA*	Citrate synthase	2.097224	1.27×10^{-20}
Cj0920c	*hisM*	Putative ABC-type amino-acid transporter permease protein	2.09015	9.49×10^{-16}
Cj0864		**Putative periplasmic protein-thioredoxin-like protein**	**2.063197**	**1.12×10^{-3}**
Cj0728		Putative periplasmic protein	2.052897	3.32×10^{-4}
Cj0917c	***cstA***	**Carbon starvation protein A**	**2.017821**	**6.06×10^{-21}**
Cj0979c		Putative secreted nuclease	1.958595	5.65×10^{-8}
Cj0156c		Ribosomal RNA small subunit methyltransferase E	1.919746	1.64×10^{-5}
Cj0528c	*flgB*	Flagellar basal body rod protein	1.882962	1.65×10^{-23}
Cj1107	*clpS*	ATP-dependent Clp protease adapter protein	1.869786	1.03×10^{-6}
Cj0429c		Uncharacterized protein	1.863965	2.77×10^{-12}
Cj1464	*flgM*	Flagellar biosynthesis protein	1.844621	7.16×10^{-11}
Cj0580c	*hemN*	Heme chaperone	1.842605	8.88×10^{-3}
Cj0922c	*PEB1C*	Aspartate/glutamate/glutamine transport system ATP-binding protein	1.836333	8.68×10^{-21}
Cj0949c		peptidyl-arginine deiminase; involved in Arginine and proline metabolism	1.829841	6.17×10^{-7}
Cj1495c		Uncharacterized protein	1.805563	5.34×10^{-24}
Cj0959c		Membrane protein insertion efficiency factor	1.783311	6.27×10^{-3}
Cj0872	***dsbA***	**Thiol:disulfide interchange protein**	**1.769298**	**2.13×10^{-4}**

Table 1. *Cont.*

Gene ID	Gene Name	Description of Product	Log^2 Fold Change	Adjusted *p*-Value
		Upregulated		
Cj0898		Histidine triad (HIT) family protein	1.748533	1.21×10^{-7}
Cj1563c		Putative transcriptional regulator	1.743043	1.47×10^{-3}
Cj1462	*flgI*	Flagellar P-ring protein	1.741476	2.47×10^{-11}
Cj1681c	*cysQ*	CysQ protein-amino acid metabolism	1.732868	7.20×10^{-4}
Cj0573		GatB/YqeY family protein	1.705464	5.93×10^{-5}
Cj0175c	*cfbpA*	Iron-uptake ABC transporter substrate-binding protein	1.694355	2.13×10^{-3}
Cj0420		Periplasmic protein	1.688196	4.43×10^{-8}
Cj0509c	***clpB***	**Stress-induced multi-chaperone system**	**1.674056**	$\mathbf{1.11 \times 10^{-10}}$
Cj1463	*flgI*	Flagellar biosynthesis protein	1.658851	2.68×10^{-6}
Cj0540		Exporting protein	1.647181	1.42×10^{-7}
Cj1025c		Uncharacterized protein	1.631584	2.18×10^{-7}
Cj1380	*dsbC*	Periplasm bi-functional thiol oxidoreductase	1.631086	8.26×10^{-16}
Cj1383c		Uncharacterized protein	1.628912	1.77×10^{-4}
Cj1382c	*fldA*	Flavodoxin I	1.599526	8.35×10^{-13}
Cj0428		Uncharacterized protein	1.589477	1.56×10^{-22}
Cj0076c	*lctP*	L-lactate transporter permease	1.57782	1.97×10^{-9}
Cj0398	*gatC*	Glutamyl-tRNA (Gln) aminotransferase subunit C	1.564965	1.01×10^{-4}
Cj0465c	***ctb***	**Group 3 truncated hemoglobin**	**1.547660**	$\mathbf{1.76 \times 10^{-5}}$
Cj1338c	*flaB*	Flagellin B	1.543761	3.16×10^{-11}
Cj1199		Putative iron/ascorbate-dependent oxidoreductase	1.535012	1.60×10^{-10}
Cj1189c	*cetB*	Bipartate energy taxis response protein	1.529662	1.76×10^{-5}
Cj1094c	*yajC*	Preprotein translocase accessory complex subunit	1.523906	3.14×10^{-5}
Cj0547	*flaG*	Flagellar protein	1.52304	4.91×10^{-4}
Cj1670c	*cgpA*	N-acetylgalactosamine (GalNAc)-containing glycoprotein	1.518031	2.82×10^{-3}
Cj1106		Thioredoxin-Single domain hemoglobin	1.500635	4.56×10^{-9}
		Downregulated		
Cj0620		**Uncharacterized protein**	**−4.25725**	2.28×10^{-3}
Cj0637c	***mrsA***	**Catalyzes the reversible oxidation-reduction of methionine sulfoxide to methionine**	**−3.94117**	$\mathbf{4.67 \times 10^{-5}}$
Cj1276c		**Integral membrane protein**	**−3.78944**	$\mathbf{8.12 \times 10^{-3}}$
Cj1282	***mrdB***	**Rod shape-determining protein**	**−3.76646**	$\mathbf{8.31 \times 10^{-3}}$
Cj1493c		Integral membrane protein	−3.41854	5.51×10^{-3}
Cj0648		Membrane protein	−3.30497	7.05×10^{-3}
Cj1080c	*hemD*	Uroporphyrinogen-III synthase	−3.29741	6.57×10^{-3}
Cj1132c		Uncharacterized protein	−2.68281	6.86×10^{-6}
Cj1448c	***kpsM***	**Capsule polysaccharide export system inner membrane**	**−2.53961**	$\mathbf{1.35 \times 10^{-6}}$
Cj1423c	*hddC*	D-glycero-alpha-D-manno-heptose 1-phosphate guanylyl transferase	−2.17572	7.22×10^{-4}
Cj0267c		Integral membrane protein	−2.08538	2.86×10^{-6}
Cj0773c		Methionine transport system permease protein	−2.0194	9.28×10^{-11}
Cj0644		TatD-related deoxyribonuclease	−1.9908	9.34×10^{-5}
Cj1567c	*nuoM*	NADH dehydrogenase I chain M	−1.9148	5.20×10^{-5}
Cj0944c		Periplasmic protein	−1.78725	2.43×10^{-3}
Cj0935c		Putative sodium:amino-acid symporter family protein	−1.77122	2.23×10^{-4}
Cj1264c	*hydD*	Putative hydrogenase maturation protease	−1.74266	1.73×10^{-6}
Cj0357c	*plsY*	Acyl phosphate: glycerol−3-phosphate acyltransferase	−1.69479	3.97×10^{-3}
Cj0411		ATP/GTP binding protein	−1.67294	1.76×10^{-5}
Cj0717		ArsC family protein	−1.64102	5.36×10^{-5}
Cj1388		Endoribonuclease L-PSP	−1.60661	2.64×10^{-3}
Cj1205c	*radA*	DNA repair and recombination	−1.51410	9.99×10^{-8}

Log^2 Fold change cut-off = >1.5. Adjusted *p*-value cut-off = <0.001. Genes highlighted in bold were chosen for RT-PCR. Annotations for Table 1 were based on NCBI reference sequence annotations (https://www.ncbi.nlm.nih.gov/refseq/, accessed on 1 August 2022). References indicate where annotations were obtained. For the complete dataset, see Supplementary Table S1.

To verify our RNA-Seq results, RNA was extracted independently of the RNA-Seq experiments for real-time RT-PCR. The first genes were *cgb* which encode a single-domain hemoglobin and *ctb* which encode a truncated hemoglobin from group III of globins; both have a major role in mediating protection of *C. jejuni* against nitric oxide and nitrosative stress [39]. *dsbA* and *dsbB* both encode periplasmic thiol oxidoreductases that repair disulfide bond in proteins that have been damaged under stress [40–42]; *cstA*, encode carbon starvation protein A; *clpB* encode an ATP-dependent protease, and *grpE* encode a heat-shock protein; all of which are involved in *C. jejuni* stress response and niche adaptation [43,44]. We also determined the expression of *peb1A*, which encodes an amino-acid binding protein in addition to facilitating cell adhesion [45], and the expression of *Cj0971*, which encodes an uncharacterized protein. A BLAST (https://blast.ncbi.nlm.nih.gov/) accessed on 1 August 2022) search of *Cj0971* protein sequence revealed the product of *Cj0971* as a filamentous hemagglutinin; this product mediates adhesion and invasion into host cells in other bacteria [46].

We also determined the expression of *ciaC* and *ciaI* encoding Campylobacter invasion antigens, both of which are essential for invasion and survival within host cells in vitro [47,48]. *kpsM* encodes a transport permease protein that is important for transportation of the capsular polysaccharide across the inner membrane, and its mutation leads to non-encapsulated *C. jejuni* [49]; *mrsA* encodes a methionine sulfoxide reductase, involved in oxidative stress repair of proteins containing methionine [50]; *mrdB* encodes a rod determining protein (RodA). Mutation to *rodA* leads to loss of rod shape in bacilli bacteria [51], and *Cj1276c* encodes an uncharacterized protein.

cgb and *ctb* had significantly increased transcripts in the RNA-Seq results; real-time RT-PCR indicated a significant ($p < 0.05$) ∼4.12-fold and a non-statistically significant ∼1.95-fold increase in expression, respectively. The two thiol oxidoreductases (*dsbA* and *dsbB*) also showed significant increase in expression in the RT-PCR experiments (∼2.74-fold and ∼2.25-fold, respectively) in line with the RNA-Seq results. *cstA*, *clpB,* and *grpE* were all significantly transcribed in the RNA-Seq results, and RT-PCR showed a significant increased expression of *cstA* (∼2.74-fold), *grpE* (∼2.39-fold), and a non-statistically significant increase in expression of *clpB* (∼1.94-fold). In line with our RNA-Seq results, *peb1A* (∼2.79-fold), *ciaC* (∼3.14-fold), *ciaI* (∼2.10-fold), and *Cj0971*(∼2.29-fold) were all significantly expressed. *kpsM* (∼−2.58-fold), *mrdB* (∼−2.55-fold), and *Cj1276c* (∼2.44-fold) were all significantly downregulated in our RT-PCR results, whilst *mrsA* (∼−1.41-fold) had a non-statistically significant reduction; this was reflective of our RNA-Seq results (Figure 4a).

Our RNA-Seq data revealed genes that were previously identified to be important during interactions of *C. jejuni* with its warm-blooded hosts but also genes that may be required during *C. jejuni* survival within amoebae host. Therefore, we generated 13 mutants in *C. jejuni* strain 11168H (Supplementary File S1: Table S2) that showed differential expression from our newly generated RNA-Seq data. We then tested their roles in survival within *A. castellanii* by enumerating CFU at 4 h post infection (Figure 4b). We chose to test *cgb*, *clpB*, *cstA*, *flgB*, *dsbA*, *dsbB*, *dsbC*, *flaA* (although this gene did not make the >1.5-fold cutoff, it was upregulated in our RNA-seq by ∼1.46-fold), *flaB*, *kpsM, mrdB, Cj0420,* and *Cj0979c* mutants.

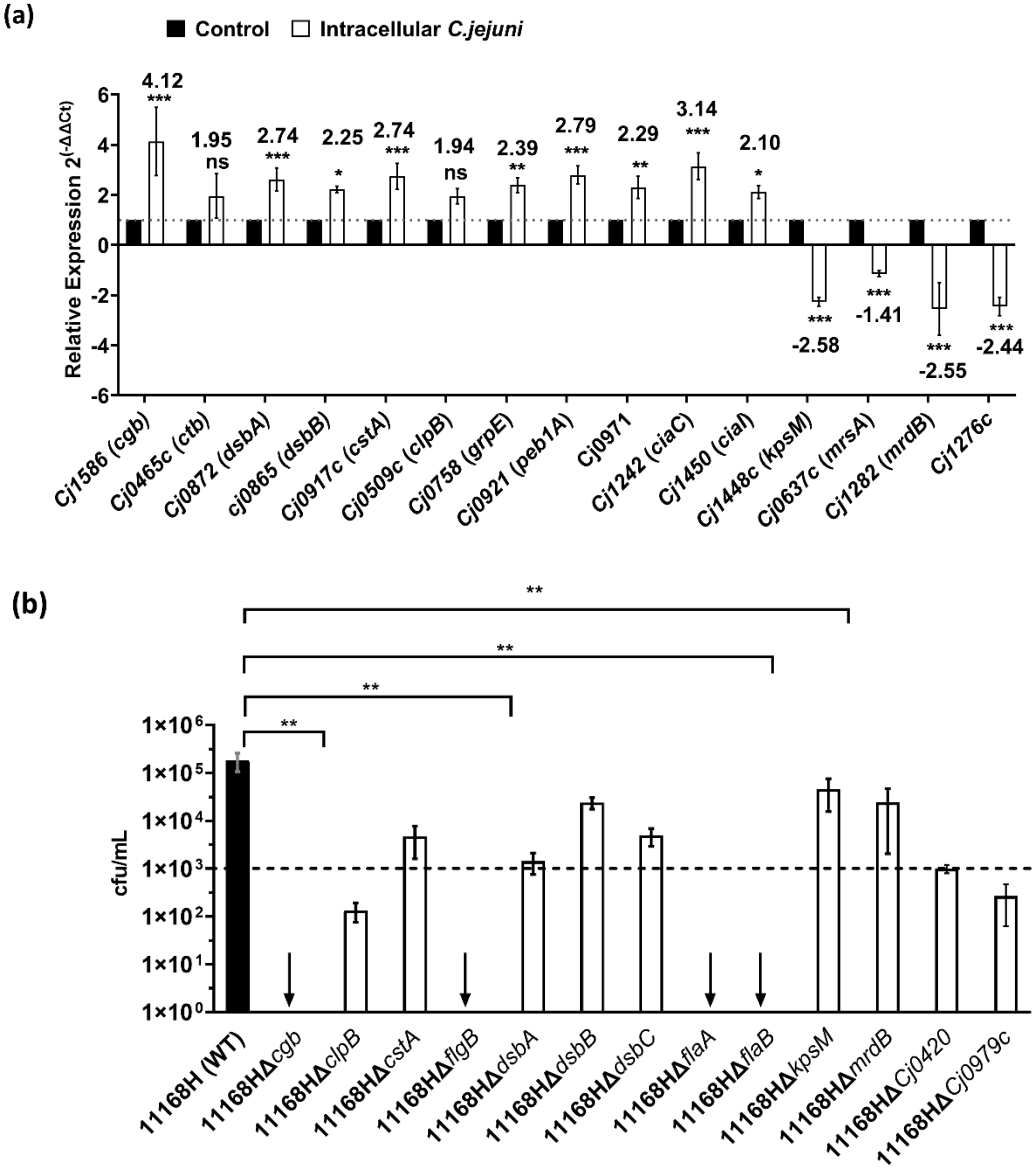

Figure 4. (**a**) **Relative gene expression of intra-amoebae *C. jejuni* 11168H.** Expression of *cgb*; *ctb*; *dsbA*; *dsbB*; *cstA*; *clpB*; *grpE*; *peb1A*; cj0971; *ciaC*; *ciaI*; *kpsM*; *mrsA*; *mrdB;* and *cj1276c* were determined by real-time RT-PCR, and results are displayed relative to the control, after normalization using expression of *gyrA*. The values are the means of three independent experiments. Error bars indicate standard deviation; * $p \leq 0.05$, ** $p \leq 0.01$, *** $p \leq 0.001$. For primers used for RT-PCR see Supplementary Table S3. (**b**)**: Survival of *C. jejuni* 11168H and respective mutants within *A. castellanii*.** Amoebae were incubated with bacteria at an M.O.I of 1:200 for 3 h before treatment with 100 μg/mL of gentamycin for 1 h. Amoebae were lysed for enumeration of live bacteria. Data is presented as cfu/mL after 4 h intracellular survival; black bar = 11168H WT; and white bar = mutants. Error bars represent SD from three independent experiments. One-way ANOVA multiple comparison was used to test for significance; ** $p \leq 0.0001$. Dotted line indicates confidence limit; arrows indicate no growth. Complete data set which includes cfu of inoculum is presented in the Supplementary File S1 (Figure S1a).

All mutants tested showed reduced intracellular survivability within *A. castellanii* relative to the 11168H parent strain. Our analyses indicated that survival within *A. castellanii* is multifactorial; however, it is likely that some factors may favor survival within amoebae more than *C. jejuni* warm-blooded hosts. Interestingly, mutation to *cgb*, *flgB* (Flagellar basal

body rod protein), *flaA* (major flagellin), and *flaB* (minor flagellin) showed no survival within *A. castellanii*. To test whether this reduction was influenced by amoebal uptake, we enumerated bacteria prior to gentamycin treatment (Supplementary File S1; Figure S1b). Our results show that whilst 11168HΔ*cgb* uptake by amoebae was similar to the WT levels, mutation to *flgB*, *flaA,* and *flaB* showed reduced uptake by *A. castellanii*, revealing the importance of an intact flagellar during amoebae interaction.

4. Discussion

Campylobacter jejuni is the leading cause of foodborne gastroenteritis [1,2]. Understanding its interactions with ubiquitous free-living amoeba in the environment is important and this may shed light on pre-adaptation to survival and virulence mechanisms required when *C. jejuni* encounters warm-blooded avian or mammalian hosts.

In this study, we investigated the interactions of *C. jejuni* 11168H with *A. castellanii* at the single-cell level. We present evidence of previously unreported interactions and propose part of the *C. jejuni*'s evolution and life-cycle is cohabitation with free-living protist (Figure 5). *C. jejuni* enters the trophozoites phago–endosomal pathway through phagocytosis; a fraction of the bacteria resists amoebal digestion and they are exocytosed. Previously, we reported that *C. jejuni* 11168H was more invasive of mammalian cells and more resistant to killing subsequent to transient internalization by *Acanthamoebae* spp. Here, our observation reveals that these more persistent bacteria are also capable of withstanding amoebal encystation.

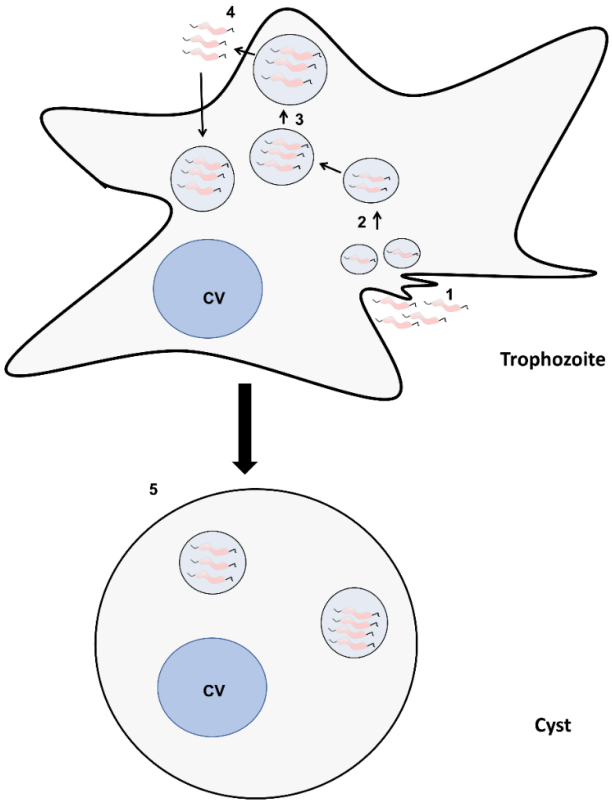

Figure 5. Scheme summarizing the interaction of *C. jejuni* 11168H with *A. castellanii*. (**1**) After internalization by amoebae trophozoites, *C. jejuni* are trafficked into tightly packed vacuoles; (**2**) which fuse into; (**3**) larger vacuoles which are emptied through exocytosis; (**4**) undigested *C. jejuni*, which are more invasive and more resistant to intracellular stresses [12], are capable of re-invading *A. castellanii*; (**5**) and occasionally these more invasive and resistant *C. jejuni* can withstand encystment of amoebae. CV = contractile vacuole.

Legionella pneumophila and *Vibrio cholerae* are known to multiply within *Acanthamoebae* spp. and even survive long-term within amoebic cysts [52,53]. Additionally, *V. cholerae* was shown to multiply within *A. castellanii* cysts, which ultimately leads to the destruction of the amoebic cell [53]. Some studies have reported multiplication of *C. jejuni* within amoebae [11,54] and destruction of amoebic cells through lysis [8]. We did not observe multiplication of *C. jejuni* 11168H in our model; however, we observed that long-term co-incubation of *C. jejuni* 11168H with amoebae led to transformation of amoebal trophozoites to cysts, which contained GFP producing *C. jejuni*. To our knowledge, this is the first study that shows evidence of *C. jejuni* within amoebae cysts. The cystic stage of amoeba is known to remain dormant for years and withstand diverse environmental stresses [19,55]. It is plausible that amoebic cysts may offer *C. jejuni* extra protection from environmental elements, this particular interaction has been reported in *L. pneumophila* [56]. We speculate that, following favorable conditions such as transmission to a host (avian or mammalian), this "Trojan horse" would transform into trophozoites potentially leading to the release of its bacteria cargo. However, at this point, it is unclear whether encystment is actively induced by *C. jejuni*. Additionally, we do not exclude that some other *C. jejuni* strains may behave differently during interactions with *Acanthamoebae* spp.; indeed, previously we showed interactions of *C. jejuni* with amoebae was not only strain dependent but also host cell dependent [12].

The transient internalization of *C. jejuni* in amoebae has the potential to extend our understanding of how this important pathogen interacts with its natural avian and mammalian hosts. Our transcriptome data of intra-amoebal bacteria suggested that *C. jejuni* utilizes similar factors to interact and survive within amoebae as it does with its natural hosts, adding weight to our previous hypothesis [12]. Similar to the interactions with its natural host [57,58], the nitrosative stress response genes, *cgb* and *ctb*, were among the most abundant transcripts in intra-amoebal *C. jejuni*, indicating nitric oxide ($NO^{\bullet}$) response. $NO^{\bullet}$ is an antimicrobial agent and an important component of the host immune system [59,60]. Disruption of *C. jejuni cgb* showed significant ($p < 0.05$) reduction in survival in our model, emphasizing the importance of $NO^{\bullet}$ defense, but also similarities between *A. castellanii* and *C. jejuni* warm-blooded hosts.

Survival and persistence within a host depends upon sensing stress and responding accordingly [61]. Our data also showed upregulation of the stress response in intra-amoebal *C. jejuni*, particularly gene products associated with DnaK, which are involved in suppressing protein aggregation consequently to environmental stress and are important to *C. jejuni* niche adaptation [57,62–64]. Other upregulated proteostasis genes were of the thiol–disulfide interchange system that repairs protein disulfide bonds, including redox stress [65]. This system is also important during *C. jejuni* interaction with its hosts [57,62,66,67], and mutation to *dsbABC* showed reduced survivability in our amoebae model. Motility and taxis are also indispensable determinants of invasion and survival within *C. jejuni* warm-blooded hosts [23,68,69]; our RNA-Seq data showed that some of the key genes involved in biosynthesis and maintenance of the flagellar were up-regulated. Disruption of *flgB* and the two heavily O-glycosylated flagellins, *flaA* and *flaB,* the former of which was shown to be involved in host cell invasion [70], showed decreased invasion to *A. castellanii*. Additionally, mutation to *flgB* was previously shown to be important in the secretion of campylobacter invasion antigens and other modulatory proteins through the putative flagellar-type 3 secretion system (FT3SS) [47,48,71]. This interesting find suggests that internalization by *A. castellanii* is partly bacterial dependent and emphasizes the importance of a fully intact and functional flagellar in *C. jejuni*-host interaction [72]. Whether it is motility, per se, and/or the non-motility properties of the *C. jejuni* flagellar that are important for these interactions, remains to be fully evaluated.

C. jejuni has a plethora of nutrient uptake and transport systems [57,62,73], which are complemented by the central carbon metabolism and electron transport system. We observed differential expression of these genes, indicating that intra-amoebic *C. jejuni* finely tunes its metabolic requirements to adapt to this niche. Both transient and obligate

intracellular pathogens are characterized by their differential expression of their metabolic needs [74,75]. We observed increased up-regulation of metabolic genes in the intra-amoebic *C. jejuni* relative to the control, indicating that the intracellular environment of *A. castellanii* is nutrient-restrictive. This was further supported by the up-regulation of the energy taxis signaling response system, *cetB* [62,76].

We also observed significant differential expression of uncharacterized genes; given that some of these genes were highly upregulated, they might be of functional importance to the transient intracellular lifestyle of *C. jejuni,* and characterization of their products might be key to advancing our understanding of this enigmatic pathogen. The novel observation that amoebae are capable of harboring *C. jejuni* 11168H necessitates further investigation on the survival of this pathogen outside the warm-blooded host. This study highlights that amoebae and *C. jejuni* warm-blooded hosts have similar properties, which makes *A. castellanii* a useful model to study *C. jejuni*-host interactions.

Supplementary Materials: The following supporting information can be downloaded at: https://www.mdpi.com/article/10.3390/microorganisms10101894/s1, Figure S1: Survival of *Campylobacter jejuni* 11168H and respective mutants within *Acanthamoeba castellanii*; Figure S2: Survival of *E. coli* Dh5$\alpha_{mCherry}$ within *A. castellanii*; Table S1: Differential expression of gene in intra-amoebae C. jejuni compared to the control in strain 11168H after 4 hr post infection; Table S2: Table of all the strain used in this study; Table S3: Primers used for RealTime RT-qPCR; Supplementary File S1: Survival of *Campylobacter jejuni* 11168H in *Acanthamoebae castellanii* provides mechanistic insight into host pathogen interactions; Movie S1: Exocytosis of *C. jejuni*.

Author Contributions: F.N. conceived the study. F.N. designed the study. M.F.H. performed survival assay. F.N. performed all other experiments. B.L. performed RNA-Seq data analysis. F.N. and B.W.W. drafted the manuscript. B.L., M.F.H. and R.A.S. edited the manuscript. All authors have read and agreed to the published version of the manuscript.

Funding: This work was supported by Biotechnology and Biological Sciences Research Council Institute Strategic Program BB/R012504/1 constituent project BBS/E/F/000PR10349 to B.W.W.

Data Availability Statement: The data that supports the RNA-Seq findings of this study are available in the Gene Expression Omnibus (GEO) under data set identifier GSE206909.

Acknowledgments: We thank Elizabeth McCarthy of the Wolfson Cell Biology Facility (WCBF) at LSHTM for providing training and technical assistance with the inverted Zeiss LSM880 confocal microscope. We thank Aidan J. Taylor for providing us with mutant constructs and Ana T. López-Jiménez for her advice.

Conflicts of Interest: The authors declare that the research was conducted in the absence of any commercial or financial relationships that could be construed as a potential conflict of interest.

References

1. Igwaran, A.; Okoh, A.I. Human campylobacteriosis: A public health concern of global importance. *Heliyon* **2019**, *5*, e02814. [CrossRef] [PubMed]
2. Elmi, A.; Nasher, F.; Dorrell, N.; Wren, B.; Gundogdu, O. Revisiting *Campylobacter jejuni* Virulence and Fitness Factors: Role in Sensing, Adapting, and Competing. *Front. Cell. Infect. Microbiol.* **2021**, *10*, 607704. [CrossRef] [PubMed]
3. Joshua, G.W.P.; Guthrie-Irons, C.; Karlyshev, A.V.; Wren, B.W. Biofilm formation in *Campylobacter jejuni*. *Microbiology* **2006**, *152*, 387–396. [CrossRef]
4. Reuter, M.; Mallett, A.; Pearson, B.M.; van Vliet, A.H.M. Biofilm Formation by *Campylobacter jejuni* Is Increased under Aerobic Conditions. *Appl. Environ. Microbiol.* **2010**, *76*, 2122–2128. [CrossRef] [PubMed]
5. Frirdich, E.; Biboy, J.; Pryjma, M.; Lee, J.; Huynh, S.; Parker, C.T.; Girardin, S.E.; Vollmer, W.; Gaynor, E.C. The *Campylobacter jejuni* helical to coccoid transition involves changes to peptidoglycan and the ability to elicit an immune response. *Mol. Microbiol.* **2019**, *112*, 280–301. [CrossRef]
6. Ikeda, N.; Karlyshev, A.V. Putative mechanisms and biological role of coccoid form formation in *Campylobacter jejuni*. *Eur. J. Microbiol. Immunol.* **2012**, *2*, 41–49. [CrossRef]
7. Lv, R.; Wang, K.; Feng, J.; Heeney, D.D.; Liu, D.; Lu, X. Detection and Quantification of Viable but Non-culturable *Campylobacter jejuni*. *Front. Microbiol.* **2020**, *10*, 2920. [CrossRef]
8. Axelsson-Olsson, D.; Waldenström, J.; Broman, T.; Olsen, B.; Holmberg, M. Protozoan *Acanthamoeba polyphaga* as a Potential Reservoir for *Campylobacter jejuni*. *Appl. Environ. Microbiol.* **2005**, *71*, 987–992. [CrossRef]

9. Snelling, W.J.; Stern, N.J.; Lowery, C.J.; Moore, J.E.; Gibbons, E.; Baker, C.; Dooley, J. Colonization of broilers by *Campylobacter jejuni* internalized within Acanthamoeba castellanii. *Arch. Microbiol.* **2008**, *189*, 175–179. [CrossRef]
10. Olofsson, J.; Axelsson-Olsson, D.; Brudin, L.; Olsen, B.; Ellström, P. *Campylobacter jejuni* Actively Invades the Amoeba Acanthamoeba polyphaga and Survives within Non Digestive Vacuoles. *PLoS ONE* **2013**, *8*, e78873. [CrossRef]
11. Vieira, A.; Seddon, A.M.; Karlyshev, A.V. Campylobacter–Acanthamoeba interactions. *Microbiology* **2015**, *161*, 933–947. [CrossRef] [PubMed]
12. Nasher, F.; Wren, B.W. Transient internalization of *Campylobacter jejuni* in Amoebae enhances subsequent invasion of human cells. *Microbiology* **2022**, *168*, 1143. [CrossRef] [PubMed]
13. Siddiqui, R.; Khan, N.A. War of the microbial worlds: Who is the beneficiary in Acanthamoeba-bacterial interactions? *Exp. Parasitol* **2012**, *130*, 311–313. [CrossRef] [PubMed]
14. Rayamajhee, B.; Subedi, D.; Peguda, H.; Willcox, M.; Henriquez, F.; Carnt, N. A Systematic Review of Intracellular Microorganisms within *Acanthamoeba* to Understand Potential Impact for Infection. *Pathogens* **2021**, *10*, 225. [CrossRef]
15. Snelling, W.J.; Moore, J.E.; McKenna, J.P.; Lecky, D.M.; Dooley, J.S. Bacterial–protozoa interactions; an update on the role these phenomena play towards human illness. *Microbes. Infect.* **2006**, *8*, 578–587. [CrossRef] [PubMed]
16. Guimaraes, A.J.; Gomes, K.X.; Cortines, J.R.; Peralta, J.M.; Peralta, R.H. Acanthamoeba spp. as a universal host for pathogenic microorganisms: One bridge from environment to host virulence. *Microbiol. Res.* **2016**, *193*, 30–38. [CrossRef]
17. Schuppler, M. How the interaction of Listeria monocytogenes and Acanthamoeba spp. affects growth and distribution of the food borne pathogen. *Appl. Microbiol. Biotechnol.* **2014**, *98*, 2907–2916. [CrossRef]
18. Centers for Disease Control and Prevention. Acanthamoeba. 8 February 2019.
19. Siddiqui, R.; Khan, N.A. Biology and pathogenesis of Acanthamoeba. *Parasites Vectors* **2012**, *5*, 6. [CrossRef]
20. Sandström, G.; Saeed, A.; Abd, H. Acanthamoeba-bacteria: A model to study host interaction with human pathogens. *Curr. Drug Targets* **2011**, *12*, 936–941. [CrossRef] [PubMed]
21. Vieira, A. Acanthamoeba as a Model for the Investigation of the Molecular Mechanisms of *Campylobacter Jejuni* Pathogenesis and Survival in the Environment. Ph.D. Thesis, Kingston University, Kingston, UK, September 2017.
22. Maal-Bared, R.; Dixon, B.; Axelsson-Olsson, D. Fate of internalized *Campylobacter jejuni* and Mycobacterium avium from encysted and excysted Acanthamoeba polyphaga. *Exp. Parasitol.* **2019**, *199*, 104–110. [CrossRef]
23. Burnham, P.M.; Hendrixson, D.R. *Campylobacter jejuni*: Collective components promoting a successful enteric lifestyle. *Nat. Rev. Genet.* **2018**, *16*, 551–565. [CrossRef] [PubMed]
24. Bronowski, C.; James, C.E.; Winstanley, C. Role of environmental survival in transmission of *Campylobacter jejuni*. *FEMS Microbiol. Lett.* **2014**, *356*, 8–19. [CrossRef] [PubMed]
25. Karlyshev, A.V.; Linton, D.; Gregson, N.A.; Wren, B.W. A novel paralogous gene family involved in phase-variable flagella-mediated motility in *Campylobacter jejuni*. *Microbiology* **2002**, *148*, 473–480. [CrossRef] [PubMed]
26. Wang, Y.; Taylor, D.E. Natural transformation in *Campylobacter* species. *J. Bacteriol.* **1990**, *172*, 949–955. [CrossRef] [PubMed]
27. Jervis, A.J.; Butler, J.A.; Wren, B.W.; Linton, D. Chromosomal integration vectors allowing flexible expression of foreign genes in *Campylobacter jejuni*. *BMC Microbiol.* **2015**, *15*, 230. [CrossRef]
28. Vieira, A.; Ramesh, A.; Seddon, A.M.; Karlyshev, A.V. CmeABC Multidrug Efflux Pump Contributes to Antibiotic Resistance and Promotes *Campylobacter jejuni* Survival and Multiplication in Acanthamoeba polyphaga. *Appl. Environ. Microbiol.* **2017**, *83*, 1600–1617. [CrossRef]
29. Joshi, N.; Fass, J. *Sickle: A Sliding-Window, Adaptive, Quality-Based Trimming Tool for FastQ Files*, Version 1.33. 2011.
30. Langmead, B.; Salzberg, S.L. Fast gapped-read alignment with Bowtie 2. *Nat. Methods* **2012**, *9*, 357–359. [CrossRef]
31. Trapnell, C.; Williams, B.A.; Pertea, G.; Mortazavi, A.; Kwan, G.; Van Baren, M.J.; Salzberg, S.L.; Wold, B.J.; Pachter, L. Transcript assembly and quantification by RNA-Seq reveals unannotated transcripts and isoform switching during cell differentiation. *Nat. Biotechnol.* **2010**, *28*, 511–515. [CrossRef]
32. Quinlan, A.R.; Hall, I.M. BEDTools: A flexible suite of utilities for comparing genomic features. *Bioinformatics* **2010**, *26*, 841–842. [CrossRef]
33. Doyscher, D.; Fieseler, L.; Dons, L.; Loessner, M.J. Markus Schuppler Acanthamoeba feature a unique backpacking strategy to trap and feed on L isteria monocytogenes and other motile bacteria. *Environ. Microbiol.* **2013**, *15*, 433–446. [CrossRef]
34. Samie, M.A.; Xu, H. Lysosomal exocytosis and lipid storage disorders. *J. Lipid Res.* **2014**, *55*, 995–1009. [CrossRef] [PubMed]
35. Li, L.; Chin, L.-S. The molecular machinery of synaptic vesicle exocytosis. *Experientia* **2003**, *60*, 942–960. [CrossRef] [PubMed]
36. Watson, R.O.; Galán, J.E. *Campylobacter jejuni* Survives within Epithelial Cells by Avoiding Delivery to Lysosomes. *PLoS Pathog.* **2008**, *4*, e14. [CrossRef]
37. Lam, W.W.L.; Woo, E.J.; Kotaka, M.; Tam, W.K.; Leung, Y.C.; Ling, T.K.W.; Au, S.W.N. Molecular interaction of flagellar export chaperone FliS and cochaperone HP1076 in Helicobacter pylori. *FASEB J.* **2010**, *24*, 4020–4032. [CrossRef]
38. Rajagopala, S.V.; Titz, B.; Goll, J.; Parrish, J.R.; Wohlbold, K.; McKevitt, M.T.; Palzkill, T.; Mori, H.; Finley, R.L.F.J.; Uetz, P. The protein network of bacterial motility. *Mol. Syst. Biol.* **2007**, *3*, 128. [CrossRef]
39. Pickford, J.L.; Wainwright, L.; Wu, G.; Poole, R.K. Expression and purification of Cgb and Ctb, the NO-inducible goblins of the foodborne bacterial pathogen *C. jejuni*. *Methods Enzym.* **2008**, *436*, 289–302.
40. Bocian-Ostrzycka, K.M.; Grzeszczuk, M.J.; Dziewit, L.; Jagusztyn-Krynicka, E.K. Diversity of the Epsilonproteobacteria Dsb (disulfide bond) systems. *Front. Microbiol.* **2015**, *6*, 570. [CrossRef]

41. Grabowska, A.D.; Wywiał, E.; Dunin-Horkawicz, S.; Łasica, A.M.; Wösten, M.M.S.M.; Nagy-Staroń, A.; Godlewska, R.; Bocian-Ostrzycka, K.; Pienkowska, K.; Łaniewski, P.; et al. Functional and Bioinformatics Analysis of Two *Campylobacter jejuni* Homologs of the Thiol-Disulfide Oxidoreductase, DsbA. *PLoS ONE* **2014**, *9*, e106247. [CrossRef]
42. Denoncin, K.; Collet, J.-F. Disulfide Bond Formation in the Bacterial Periplasm: Major Achievements and Challenges Ahead. *Antioxid. Redox Signal.* **2013**, *19*, 63–71. [CrossRef]
43. Alam, A.; Bröms, J.E.; Kumar, R.; Sjöstedt, A. The Role of ClpB in Bacterial Stress Responses and Virulence. *Front. Mol. Biosci.* **2021**, *8*, 668910. [CrossRef]
44. Stintzi, A. Gene Expression Profile of *Campylobacter jejuni* in Response to Growth Temperature Variation. *J. Bacteriol.* **2003**, *185*, 2009–2016. [CrossRef] [PubMed]
45. Leon-Kempis Mdel, R.; Guccione, E.; Mulholland, F.; Williamson, M.P.; Kelly, D.J. The *Campylobacter jejuni* PEB1a adhesin is an aspartate/glutamate-binding protein of an ABC transporter essential for microaerobic growth on dicarboxylic amino acids. *Mol. Microbiol.* **2006**, *60*, 1262–1275. [CrossRef] [PubMed]
46. Locht, C.; Berlin, P.; Menozzi, F.D.; Renauld, G. The filamentous haemagglutinin, a multifaceted adhesion produced by virulent *Bordetella* spp. *Mol. Microbiol.* **1993**, *9*, 653–660. [CrossRef] [PubMed]
47. Neal-McKinney, J.M.; Konkel, M.E. The *Campylobacter jejuni* CiaC virulence protein is secreted from the flagellum and delivered to the cytosol of host cells. *Front. Cell. Infect. Microbiol.* **2012**, *2*, 31. [CrossRef]
48. Buelow, D.R.; Christensen, J.E.; Neal-McKinney, J.M.; Konkel, M.E. *Campylobacter jejuni* survival within human epithelial cells is enhanced by the secreted protein CiaI. *Mol. Microbiol.* **2011**, *80*, 1296–1312. [CrossRef]
49. Karlyshev, A.V.; Linton, D.; Gregson, N.A.; Lastovica, A.J.; Wren, B.W. Genetic and biochemical evidence of a *Campylobacter jejuni* capsular polysaccharide that accounts for Penner serotype specificity. *Mol. Microbiol.* **2000**, *35*, 529–541. [CrossRef]
50. Atack, J.M.; Kelly, D.J. Contribution of the stereospecific methionine sulphoxide reductases MsrA and MsrB to oxidative and nitrosative stress resistance in the food-borne pathogen *Campylobacter jejuni*. *Microbiology* **2008**, *154*, 2219–2230. [CrossRef]
51. Jones, L.J.; Carballido-López, R.; Errington, J. Control of Cell Shape in Bacteria: Helical, Actin-like Filaments in Bacillus subtilis. *Cell* **2001**, *104*, 913–922. [CrossRef]
52. Bouyer, S.; Imbert, C.; Rodier, M.-H.; Héchard, Y. Long-term survival of Legionella pneumophila associated with *Acanthamoeba castellanii* vesicles. *Environ. Microbiol.* **2007**, *9*, 1341–1344. [CrossRef]
53. Van der Henst, C.; Scrignari, T.; Maclachlan, C.; Blokesch, M. An intracellular replication niche for Vibrio cholerae in the amoeba Acanthamoeba castellanii. *ISME J.* **2016**, *10*, 897–910. [CrossRef]
54. Axelsson-Olsson, D.; Olofsson, J.; Svensson, L.; Griekspoor, P.; Waldenström, J.; Ellström, P.; Olsen, B. Amoebae and algae can prolong the survival of *Campylobacter* species in co-culture. *Exp. Parasitol.* **2010**, *126*, 59–64. [CrossRef] [PubMed]
55. Visvesvara, G.S.; Moura, H.; Schuster, F.L. Pathogenic and opportunistic free-living amoebae: *Acanthamoeba* spp., *Balamuthia mandrillaris*, *Naegleria fowleri*, and *Sappinia diploidea*. *FEMS Immunol. Med. Microbiol.* **2007**, *50*, 1–26. [CrossRef] [PubMed]
56. Nisar, M.A.; Ross, K.E.; Brown, M.H.; Bentham, R.; Whiley, H. Legionella pneumophila and Protozoan Hosts: Implications for the Control of Hospital and Potable Water Systems. *Pathogens* **2020**, *9*, 286. [CrossRef]
57. Taveirne, M.E.; Theriot, C.M.; Livny, J.; DiRita, V.J. The Complete *Campylobacter jejuni* Transcriptome during Colonization of a Natural Host Determined by RNAseq. *PLoS ONE* **2013**, *8*, e73586. [CrossRef]
58. Hermans, D.; Van Deun, K.; Martel, A.; Van Immerseel, F.; Messens, W.; Heyndrickx, M.; Haesebrouck, F.; Pasmans, F. Colonization factors of *Campylobacter jejuni* in the chicken gut. *Veter Res.* **2011**, *42*, 82. [CrossRef] [PubMed]
59. Vazquez-Torres, A.; Stevanin, T.; Jones-Carson, J.; Castor, M.; Read, R.C.; Fang, F.C. Analysis of Nitric Oxide-Dependent Antimicrobial Actions in Macrophages and Mice. *Methods Enzymol.* **2008**, *437*, 521–538. [CrossRef] [PubMed]
60. Fang, F.C. Antimicrobial reactive oxygen and nitrogen species: Concepts and controversies. *Nat. Rev. Genet.* **2004**, *2*, 820–832. [CrossRef]
61. Singh Amoolya, H.; Wolf, D.M.; Wang, P.; Arkin, A.P. Modularity of stress response evolution. *Proc. Natl. Acad. Sci. USA* **2008**, *105*, 7500–7505. [CrossRef]
62. Looft, T.; Cai, G.; Choudhury, B.; Lai, L.X.; Lippolis, J.; Reinhardt, T.; Sylte, M.J.; Casey, T.A. Avian Intestinal Mucus Modulates *Campylobacter jejuni* Gene Expression in a Host-Specific Manner. *Front. Microbiol.* **2018**, *9*, 3215. [CrossRef]
63. Santra, M.W.; Daniel, F.; Ken, A.D. Bacterial proteostasis balances energy and chaperone utilization efficiently. *Proc. Natl. Acad. Sci. USA* **2017**, *114*, E2654–E2661. [CrossRef]
64. Schramm, F.D.; Schroeder, K.; Jonas, K. Protein aggregation in bacteria. *FEMS Microbiol. Rev.* **2020**, *44*, 54–72. [CrossRef] [PubMed]
65. Nagy, P. Kinetics and Mechanisms of Thiol—Disulfide Exchange Covering Direct Substitution and Thiol Oxidation-Mediated Pathways. *Antioxid. Redox Signal.* **2013**, *18*, 1623–1641. [CrossRef] [PubMed]
66. Maskos, K.; Huber-Wunderlich, M.; Glockshuber, R. DsbA and DsbC-catalyzed oxidative folding of proteins with complex disulfide bridge patterns in vitro and in vivo. *J. Mol. Biol.* **2003**, *325*, 495–513. [CrossRef]
67. Banaś, A.M.; Bocian-Ostrzycka, K.M.; Dunin-Horkawicz, S.; Ludwiczak, J.; Wilk, P.; Orlikowska, M.; Wyszyńska, A.; Dąbrowska, M.; Plichta, M.; Spodzieja, M.; et al. Interplay between DsbA1, DsbA2 and C8J_1298 Periplasmic Oxidoreductases of *Campylobacter jejuni* and Their Impact on Bacterial Physiology and Pathogenesis. *Int. J. Mol. Sci.* **2021**, *22*, 13451. [CrossRef] [PubMed]
68. Nachamkin, I.; Yang, X.H.; Stern, N.J. Role of *Campylobacter jejuni* flagella as colonization factors for three-day-old chicks: Analysis with flagellar mutants. *Appl. Environ. Microbiol.* **1993**, *59*, 1269–1273. [CrossRef] [PubMed]
69. Guerry, P. Campylobacter flagella: Not just for motility. *Trends Microbiol.* **2007**, *15*, 456–461. [CrossRef]

70. Wassenaar, T.; Bleumink-Pluym, N.M.; Van Der Zeijst, B. Inactivation of *Campylobacter jejuni* flagellin genes by homologous recombination demonstrates that flaA but not flaB is required for invasion. *EMBO J.* **1991**, *10*, 2055–2061. [CrossRef]
71. Barrero-Tobon, A.M.; Hendrixson, D.R. Identification and analysis of flagellar coexpressed determinants Feds of *Campylobacter jejuni* involved in colonization. *Mol. Microbiol.* **2012**, *84*, 352–369. [CrossRef]
72. Konkel, M.E.; Klena, J.D.; Rivera-Amill, V.; Monteville, M.R.; Biswas, D.; Raphael, B.; Mickelson, J. Secretion of Virulence Proteins from *Campylobacter jejuni* Is Dependent on a Functional Flagellar Export Apparatus. *J. Bacteriol.* **2004**, *186*, 3296–3303. [CrossRef]
73. Cróinín, T.O.; Backert, S. Host epithelial cell invasion by *Campylobacter jejuni*: Trigger or zipper mechanism? *Front. Cell. Infect. Microbiol.* **2012**, *2*, 25. [CrossRef]
74. Best, A.; Kwaik, A.Y. Nutrition and Bipartite Metabolism of Intracellular Pathogens. *Trends Microbiol.* **2019**, *27*, 550–561. [CrossRef] [PubMed]
75. Li, H.; Limenitakis, J.P.J.; Fuhrer, T.; Geuking, M.; Lawson, M.A.; Wyss, M.; Brugiroux, S.; Keller, I.; Macpherson, J.A.; Rupp, S.; et al. The outer mucus layer hosts a distinct intestinal microbial niche. *Nat. Commun.* **2015**, *6*, 8292. [CrossRef] [PubMed]
76. Christina, S.V.; Brøndsted, L.; Li, Y.-P.; Bang, D.D.; Ingmer, H. Energy Taxis Drives *Campylobacter jejuni* toward the Most Favorable Conditions for Growth. *Appl. Environ. Microbiol.* **2009**, *75*, 5308–5314.